Journal of Biomolecular NMR, 1 (1991) 349–361
ESCOM

J-Bio NMR 032

Segmental differences in the stability of the *trp*-repressor peptide backbone

Jerzy Czaplicki, Cheryl Arrowsmith and Oleg Jardetzky*

Stanford Magnetic Resonance Laboratory, Stanford University, Stanford, CA 94305-5055, U.S.A.

Dedicated to the memory of Professor V.F. Bystrov

Received 22 May 1991
Accepted 12 August 1991

Keywords: Amide proton exchange rates; *trp*-repressor

SUMMARY

Exchange lifetimes of amide protons in *trp*-repressor with and without the corepressor, L-tryptophan, were studied by heteronuclear 2D NMR spectroscopy. The amide proton exchange times revealed pronounced differences in the stability of different regions of the *trp*-repressor. The dimeric core of the molecule is relatively compact and homogeneous in terms of the measured parameters in both apo- and holorepressors. On the other hand the DNA-binding region appears less stable and more susceptible to the exchange of its backbone protons with the solvent. The NMR findings reported here are consistent with and amplify information on the stability of the *trp*-repressor obtained by other methods.

INTRODUCTION

The *trp*-repressor from *E. coli* is an allosteric protein regulating the biosynthesis of L-tryptophan (Klig et al., 1988). The molecule is a symmetric dimer of two identical chains containing 107 residues each, with a dimer molecular weight of 25 kDa. In the absence of L-trp the (tryptophan-free) repressor molecules (aporepressor) have a low affinity for DNA. In the presence of L-trp one molecule of *trp*-repressor and two molecules of L-trp form a complex (holorepressor). This, in turn, forms a stable ternary complex with three *trp*-operator DNA sequences, thereby inhibiting the production of enzymes involved in tryptophan biosynthesis.

The structure of the *trp*-repressor is known from both crystallographic (Schevitz et al., 1985; Zhang et al., 1987; Otwinowski et al., 1988) and NMR studies (Hyde et al., 1989; Arrowsmith et al., 1989,1990a,b,1991a,b). The molecule contains 12 helices (6 per monomer, denoted by letters A–F in the order of monomer sequence) and is a member of the helix-turn-helix family of repres-

* To whom correspondence should be addressed.

sors. Four of the helices (A, B, C and F) constitute the dimeric core of the molecule while the other two (D and E) form the helix-turn-helix DNA-binding region.

In our NMR studies of the *trp*-repressor structure we have early on made the observation that more NOEs per residue could be observed for the ABCF core of the molecule than for the DE DNA-binding segment. The fact that the core and the DE regions are observed in the same sample under exactly the same experimental conditions rules out most of the instrumental reasons for the absence of NOEs and makes it necessary to look for a physical cause of this phenomenon. Even though the *relative* absence of NOEs cannot by itself be regarded as conclusive evidence for segmental mobility and averaging of interproton distances (an alternative explanation – enhanced spin diffusion – could mean quite the opposite), it nevertheless provides strong presumptive evidence for the existence of larger scale molecular motions and makes a detailed study of the dynamics necessary.

In a preliminary study of ^{15}N-labeled *trp*-repressor (Arrowsmith et al., 1991a) and observations of the amide region of the native repressor, the exchange rates could be classified into three categories: fast ($\tau_{ex} < 10$ min), intermediate ($\tau_{ex} \approx$ a few hours), and slow ($\tau_{ex} \approx$ days). Most of the rapidly exchanging protons could be assigned to the helix-turn-helix DNA-binding region. In this paper we present a more detailed study of exchange rates for individual residues of the *trp*-repressor in both the apo- and the holo-forms at 35 and 45°C. These studies have allowed us to map out the less stable regions in the protein sequence and correlate them with the secondary and tertiary structure.

MATERIALS AND METHODS

Trp-repressor was isolated from *E.coli* strain CY15070 containing the overproducing plasmid pJPR2 and purified according to Paluh and Yanofsky (1986). To ensure uniform labeling of the protein the bacteria were grown in minimal medium with $^{15}NH_4Cl$ as the only source of ^{15}N. For NMR measurements the *trp*-repressor sample was concentrated to 2 mM (in terms of protein monomer) in the NMR buffer (500 mM NaCl, 50 mM Na_2HPO_4, 90% H_2O/10% D_2O) at pH = 5.7. All measurements were performed on a Bruker AM500 spectrometer equipped with an Aspect 3000 computer and FMR decoupler tuned to the ^{15}N frequency (50.7 MHz). Spectra are referenced to internal TSP (^{1}H) and external NH_4Cl in the NMR buffer, pH = 0.6 (^{15}N). The assignments of proton signals for *trp*-holorepressor at 45°C have been published previously (Arrowsmith et al., 1990a) and those for the aporepressor are also known (Arrowsmith et al., 1991b). Assignments of the NH signals in HMQC spectra (Bax et al., 1983) at 45°C have been confirmed by 3D HMQC-NOESY spectra of the aporepressor obtained at 600 MHz. To enable us to assign cross peaks at 35°C, a series of 2D-HMQC spectra was recorded in the range 35–45°C at intermediate temperatures differing by no more than 2–3 deg and the changes in chemical shifts of individual lines were continuously monitored.

For the study of exchange rates the sample was lyophilized from H_2O solution and redissolved in D_2O. The time at which D_2O was added was taken as the beginning (time 'zero') of each experiment. 30 min were necessary for temperature stabilization, tuning and shimming, therefore the first lines to disappear in the 2D experiment must have lifetimes of less than 10 min (i.e. an exponential decay to < 10% of intensity over 30 min). A series of 2D proton-detected ^{15}N-^{1}H single-bond correlation HMQC spectra was acquired over a period of 36 h. The recording time of each

individual spectrum was kept as short as possible in order to minimize the effects of averaging caused by exchange taking place during acquisition. The obvious limiting factor was the S/N ratio which had to be kept sufficiently high and the 1.5 s relaxation delay which cannot be reduced for this protein. Typically one 2D spectrum could be recorded in ca. 3 h. Spectral widths of 6 kHz in F_2 and 3 kHz in F_1 were used, with 1K data points in t_2 and 200 t_1 slices of 32 scans each. The water resonance was suppressed using coherent presaturation during the relaxation delays. For data processing zero filling was used to 2K in F_2 and to 1K in F_1. Data points were apodized in both dimensions with squared sine-bell windows shifted by 45°. The intensities of individual lines in 2D spectra were monitored as a function of time.

Evaluation of numerical results from the exchange data requires caution as the intensities of many of the signals change markedly during acquisition of a single 2D spectrum. In order to facilitate the quantitative analysis of the results the following expression has been derived that describes the averaged amplitude A_{ex} of a Lorentzian line in a 2D spectrum under the influence of the exchange effect:

$$A_{ex}(\omega_1,\omega_2)=A_0 e^{-t_0/\tau}\cdot\left\{\frac{\tau}{t_a}(1-e^{-t_a/\tau})\cdot\frac{T_2^{*1}}{\left[1+\left(\frac{t_a\cdot T_2^{*1}}{\tau\cdot\Delta t_1}\right)\right]\left[1+\left(\frac{\omega_1-\omega_1^0}{\frac{1}{T_2^{*1}}+\frac{t_a}{\tau\cdot\Delta t_1}}\right)^2\right]}\cdot\right.$$

$$\left.\frac{T_2^{*2}}{\left[1+\left(\frac{T_2^{*2}}{\tau}\right)\right]\left[1+\left(\frac{\omega_2-\omega_2^0}{\frac{1}{T_2^{*2}}+\frac{1}{\tau}}\right)^2\right]}\right\} \qquad (1)$$

where A_0 is the amplitude of the line, t_a is the acquisition time of an FID, τ is the time constant describing the exchange lifetime, Δt_1 is the increment (dwell time) in the t_1 dimension, T_2^{*i} denotes the effective transverse relaxation time in dimension t_i ($i=1,2$), ω_i and ω_o^i are running frequency and frequency of the center of a line in dimension t_i, respectively, and t_o is the time elapsed from the beginning of the experiment after which the acquisition of a particular 2D spectrum has begun. The exponential dependence of (1) on t_o with τ being the time constant allows one to extract τ from a *series* of 2D spectra acquired for different t_o's.

The ^{15}N-T_1, T_2 and $T_{1\rho}$ relaxation times were measured using pulse sequences described in Kay et al. (1989). They are not reported here in detail because of uniformity of their values for all the molecule. However, these results proved to be useful in supporting the exchange data by supplying the lower limits on exchange times.

RESULTS AND DISCUSSION

As already noted in the Introduction, our first unusual NMR observation on the *trp*-repressor was the *relative* scarcity of NOEs in the putative DNA-binding region, helices D and E for the

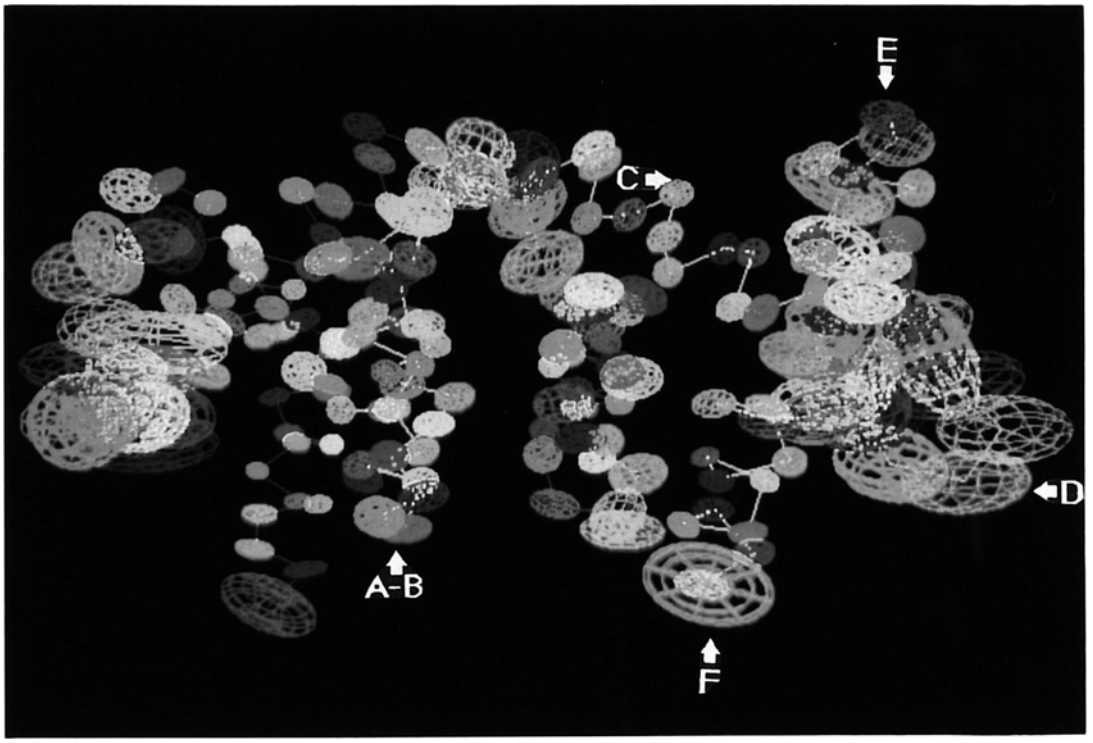

Fig. 1. A computer-generated structural model of a *trp*-repressor molecule. The C^{α} backbone trace of the *trp* holorepressor dimer has been determined from NOE data (Arrowsmith et al., 1991b). The colored spheres represent the uncertainty in atomic position and their radius is drawn at 2 SD.

aporepressor (Arrowsmith et al., 1991b) and helix D for the holorepressor (Arrowsmith et al., 1990a). This finding was clearly reflected in structure calculations. Since our method of structure calculation, based on the Kalman filter allows a direct estimate of uncertainty in atomic positions implied by the data (Altman and Jardetzky, 1989; Pachter et al., 1991), a dramatic difference in the precision to which the backbone coordinates could be defined for different parts of the molecule could be seen. Figure 1 shows this result for the holorepressor, in which the uncertainties of atomic positions for the D helix are much larger than those for the dimeric core of the molecule. For the aporepressor both the D and E regions remain relatively ill-defined. This finding prompted a more detailed investigation of the dynamics of different segments of *trp*-repressor. The data reported here support the interpretation that the observed differences in precision with which different parts of the molecule can be defined reflect differences in flexibility.

Figure 2 shows the result of a typical HMQC exchange experiment on the *trp*-holorepressor at 35°C. The assignments of the nitrogen chemical shifts are given in Table 1. Under the best conditions a total of 102 amide proton correlations could be observed in H_2O corresponding to the 107 amino acids in the monomer less 4 prolines and the N-terminal Ala. A total of 77 of these could be assigned based on previously assigned proton chemical shifts and a 3D HMQC-NOESY experiment. Of the assigned peaks, approximately 10–15% (depending on conditions) were partially

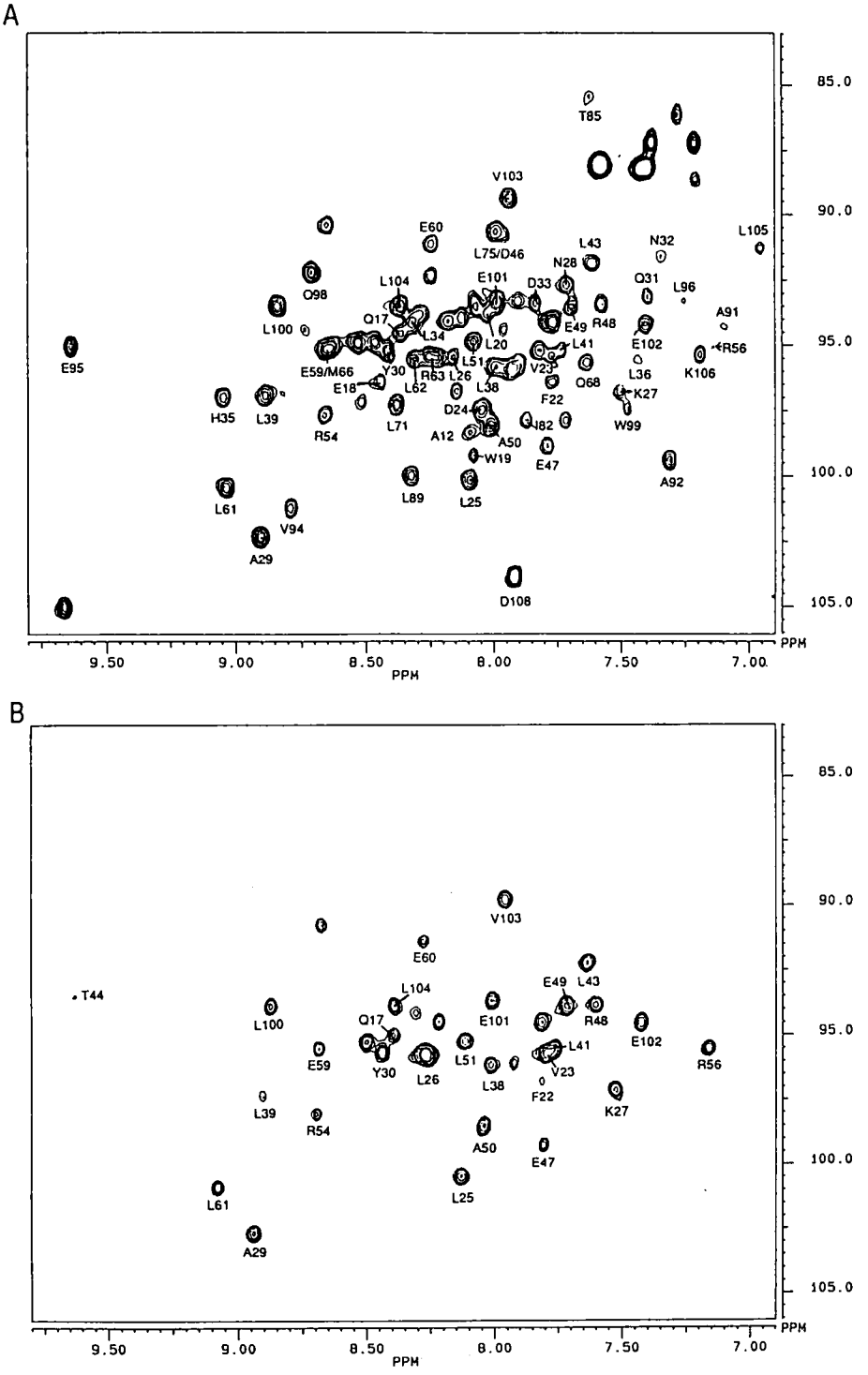

Fig. 2. A comparison between the HMQC spectrum of the *trp* holorepressor in H_2O at 45°C (A) and an HMQC taken 30 min after dissolving in D_2O (B).

TABLE I
^{1}H AND ^{15}N CHEMICAL SHIFTS OF ASSIGNED *trp*-REPRESSOR RESIDUES

Residue	^{1}H (ppm) at 45°C[a]		^{15}N (ppm) at 45°C[b]	
	Apo[c]	Holo[d]	Apo	Holo
Ala[12]		8.19	98.40	98.50
Glu[13]		8.29		
Gln[14]		8.22		
Arg[15]				
His[16]	8.29	8.34	95.78	
Gln[17]	8.34	8.34	94.33	94.78
Glu[18]	8.43	8.43	96.44	96.58
Trp[19]	8.09	8.09	99.28	99.28
Leu[20]	7.99	7.99	93.90	94.00
Arg[21]				
Phe[22]	7.84	7.78	96.70	96.54
Val[23]	7.78	7.78	97.13	95.56
Asp[24]	8.05	8.05	97.71	97.52
Leu[25]	8.10	8.10	100.16	100.26
Leu[26]	8.22	8.22	97.03	95.70
Lys[27]	7.49	7.49	96.74	96.93
Asn[28]	7.71	7.71	92.92	92.86
Ala[29]	8.89	8.89	102.41	102.51
Tyr[30]	8.40	8.40	97.23	95.37
Gln[31]	7.40	7.40	93.41	93.31
Asn[32]	7.32	7.32	91.85	91.85
Asp[33]	7.88	7.88	93.61	93.61
Leu[34]	8.28	8.28	93.80	94.39
His[35]	9.02	9.02	96.93	97.23
Leu[36]	7.42	7.42	95.66	95.86
Pro[37]				
Leu[38]	7.97	7.97	95.37	95.95
Leu[39]	8.89	8.89	96.74	97.23
Asn[40]	8.18	8.18	93.22	
Leu[41]	7.51	7.69	95.56	95.37
Met[42]	8.09	8.64	96.74	
Leu[43]	7.82	7.64	93.90	92.08
Thr[44]	9.10	9.50		93.37
Pro[45]				
Asp[46]	8.04	7.95	90.87	91.03
Glu[47]	7.59	7.80	98.69	99.08
Arg[48]	7.82	7.57	94.49	93.64
Glu[49]	7.77	7.70	93.90	93.64
Ala[50]	7.93	8.04	98.11	98.20
Leu[51]	8.10	8.10	95.56	97.17
Gly[52]	8.20	8.13	80.90	
Thr[53]	8.26	8.03		
Arg[54]	8.63	8.63	97.91	97.91
Val[55]	7.85	7.78	95.17	94.39
Arg[56]	7.22	7.08	95.66	95.27
Ile[57]	8.16	8.35	93.41	
Val[58]	8.05	8.46		

TABLE 1 (continued)

Residue	^{1}H (ppm) at 45°C[a]		^{15}N (ppm) at 45°C[b]	
	Apo[c]	Holo[d]	Apo	Holo
Glu[59]	8.45	8.65	95.27	95.41
Glu[60]	8.25	8.25	91.94	91.46
Leu[61]	8.82	9.00	99.67	100.65
Leu[62]	8.28	8.28	95.76	95.56
Arg[63]	8.24	8.24		95.47
Gly[64]	7.70	7.63	79.90	
Glu[65]	7.82	7.82		
Met[66]	8.49	8.60	95.37	95.31
Ser[67]	8.70	8.13	93.80	
Gln[68]	7.78	7.65	95.76	95.76
Arg[69]	8.21	8.37	94.72	
Glu[70]	7.93	7.93	96.11	
Leu[71]			97.32	97.42
Lys[72]				
Asn[73]	7.95	7.83	95.90	
Glu[74]	8.54	8.54	95.33	
Leu[75]	7.99	7.99	92.63	91.03
Gly[76]	7.87	7.87	84.50	
Ala[77]	7.36	7.01	99.18	
Gly[78]	8.29	8.29		
Ile[79]		8.29		
Ala[80]		8.08		
Thr[81]	7.58	7.58	90.52	
Ile[82]	7.90	7.90	98.50	98.00
Thr[83]		8.50	91.34	
Arg[84]		7.68		
Gly[85]		7.61		85.78
Ser[86]		8.24		
Asn[87]	7.84	8.40		
Ser[88]		8.06		
Leu[89]	8.30	8.30	99.67	100.10
Lys[90]	7.81	7.74	94.49	
Ala[91]	7.28	7.09	94.88	94.49
Ala[92]	7.31	7.31	99.18	99.51
Pro[93]				
Val[94]	8.80	8.80	101.33	101.33
Glu[95]	9.62	9.62	95.17	95.37
Leu[96]	7.24	7.24	93.61	93.65
Arg[97]	7.89	7.89	95.76	95.99
Gln[98]	8.70	8.70	92.24	92.53
Trp[99]	7.48	7.48	97.52	97.50
Leu[100]	8.83	8.83	93.61	93.70
Glu[101]	7.99	7.99	93.51	93.61
Glu[102]	7.41	7.41	94.33	94.39
Val[103]	7.93	7.93	89.66	89.70
Leu[104]	8.35	8.35	93.61	93.74
Leu[105]	7.12	7.12	91.65	91.36
Lys[106]	7.19	7.19	95.50	95.52

TABLE 1 (continued)

Residue	^{1}H (ppm) at 45°C[a]		^{15}N (ppm) at 45°C[b]	
	Apo[c]	Holo[d]	Apo	Holo
Ser[107]				
Asp[108]	7.92	7.92	103.78	103.97

[a] ±0.03 ppm.
[b] ±0.1 ppm.
[c] from Arrowsmith et al., 1991b.
[d] from Arrowsmith et al., 1990a.

overlapping or of such weak intensity even in H_2O that accurate rates could not be obtained. In general there is more spectral dispersion in spectra of the holorepressor. The low-intensity peaks could be due either to inherently broad lines, or saturation transfer via rapid exchange with the solvent which was presaturated.

The exchange lifetimes for assigned residues at 35 and 45°C are given in Table 2. An upper limit on exchange time of 10 min was estimated for signals that were observed in HMQC spectra in H_2O but whose exchange times were short enough to preclude observation in the first exchange spectrum. A lower time limit of about 5 s could be estimated from relaxation experiments. The time window of the experiment did not allow us to make extrapolations of exchange times for the slowest protons and consequently the corresponding bars are broken at 100 h. However, many of these lifetimes may be of the order of 500 h, as was found for some of the leucines (Arrowsmith et al., 1991b).

As in the previous report (Arrowsmith et al., 1991a), three fractions of protons were observed. For the aporepressor approximately 57% of the assigned and resolved protons exchanged very rapidly, so that the corresponding peaks could not be seen even in the first exchange spectrum; a second small fraction (ca. 20%) exchanged gradually within hours while the remaining 23% were present over a period of days at 35°C. Most of the unassigned peaks exchanged very fast, with only 5–6 slowly exchanging peaks left unassigned.

L-trp binding causes the exchange times for the holorepressor to be longer than those for the aporepressor by a factor of between 3 (at 35°C) and 10 (at 45°C). The exchange times exhibit a strong temperature dependence. Exchange times decrease by ~ 1–2 orders of magnitude on going from 35 to 45°C. It should be noted that this is not due to the onset of denaturation, which occurs at temperatures above 80°C in aqueous solutions (Lane and Jardetzky, 1987). The chemical shifts and the NOE pattern remain very similar between 35 and 45°C. For the lines that can be seen, the stabilizing effect of L-trp is still clearly observed. Unfortunately, the coalescence of NH resonances at lower temperatures and their rapid disappearance at higher temperatures has precluded the possibility of obtaining accurate values of activation energies for the exchange process.

Since the ^{15}N relaxation experiments have been carried out in H_2O, most of the backbone protons can be observed, although some remain unassigned due to spectral overlap. T_2 and $T_{1\rho}$ values of ~ 100 ms were found for the aporepressor at 45°C, indicating that the major contribution to $T_{1\rho}$ relaxation is from motions in the ns time range. For many of the fast exchanging protons T_1 values of 500–700 ms could be measured for the amide nitrogen. Hence, the exchange times for

TABLE 2
THE EXCHANGE LIFETIMES FOR ASSIGNED APO- AND HOLOREPRESSOR RESIDUES

Residue	Estimated Exchange Times (h)[a]			
	Apo		Holo	
	35°C	45°C	35°C	45°C
Ala[12]	–	re	re	re
His[16]	re	re	u	u
Gln[17]	re	re	u	u
Glu[18]	re	re	re	re
Trp[19]	re	re	re	re
Leu[20]	re	re	–	re
Phe[22]	19	2	37	5
Val[23]	> 100	12	> 100	74
Asp[24]	re	re	re	re
Leu[25]	> 100	11	> 100	19
Leu[26]	> 100	22	> 100	> 100
Lys[27]	62	5	86	16
Asn[28]	4	re	53	~ 1
Ala[29]	77	2	> 100	56
Tyr[30]	49	2	85	16
Gln[31]	re	re	re	re
Asn[32]	re	re	re	re
Asp[33]	re	re	re	re
Leu[34]	30	3.4	97	23
His[35]	re	re	re	re
Leu[36]	re	re	re	re
Leu[38]	26	–	> 100	99
Leu[39]	18	2	95	5
Asn[40]	–	2	–	–
Leu[41]	23	2	> 100	73
Leu[43]	26	3	> 100	55
Thr[44]	–	–	–	6
Asp[46]	re	re	re	re
Glu[47]	4	3	11	4
Arg[48]	–	–	> 100	> 100
Glu[49]	20	2	65	19
Ala[50]	7	2	27	1
Leu[51]	23	3	> 100	> 100
Gly[52]	u	u	39	u
Arg[54]	69	3	> 100	69
Val[55]	–	3	> 100	> 100
Arg[56]	15	3	36	24.9
Glu[59]	54	3	> 100	> 100
Glu[60]	69	2–4	> 100	> 100
Leu[61]	51	5	> 100	51
Leu[62]	68	22	> 100	> 100
Gly[64]	–	–	re	–
Met[66]	re	re	re	re
Ser[67]	re	–	u	u
Gln[68]	re	re	u	re
Arg[69]	re	re	–	u

TABLE 2 (continued)

Residue	Estimated Exchange Times (h)[a]			
	Apo		Holo	
	35°C	45°C	35°C	45°C
Glu^{70}	re	re	–	u
Leu^{71}	re	re	re	re
Asn^{73}	re	re	–	u
Glu^{74}	re	re	re	u
Leu^{75}	re	re	re	re
Gly^{76}	u	u	re	u
Ala^{77}	–	re	–	re
Gly^{78}	u	u	re	u
Ile^{79}	re	–	u	u
Thr^{81}	re	–	u	u
Ile^{82}	re	re	u	–
Gly^{85}	u	u	re	re
Asn^{87}	u	u	re	–
Leu^{89}	re	re	re	re
Lys^{90}	re	re	–	u
Ala^{91}	re	re	re	re
Ala^{92}	re	re	re	re
Val^{94}	re	re	re	re
Glu^{95}	re	re	re	re
Leu^{96}	re	re	re	re
Arg^{97}	u	re	re	re
Gln^{98}	re	re	re	re
Trp^{99}	3	re	7	4
Leu^{100}	13	2	100	35
Glu^{101}	25	2	57	13
Glu^{102}	11	2	23	5
Val^{103}	10	2	49	13
Leu^{104}	10	2	44	4
Leu^{105}	re	re	re	re
Lys^{106}	re	re	re	re
Ser^{107}	u	u	re	u
Asp^{108}	re	re	re	re

re = rapid exchange – estimated upper limit for exchange time is between 5 s and 10 min (see text for discussion).
u = unassigned.
– = not measurable due to low intensity or overlap.
[a] Estimated error is ± 10–20% for intense lines and ± 20–50% for weaker lines and those with $\tau_{ex} < 10$ h.

these residues cannot be shorter than a few seconds and at the same time they cannot be longer than approximately 10 min. Addition of L-trp has no significant effect on the measured ^{15}N relaxation times, which remain largely in the range of 500–700 ms.

Figure 3 shows the distribution of exchange lifetimes along the peptide sequence for the apo (A)- and holorepressor (B) at 35°C. The secondary structure of the repressor is also shown for comparison. It is immediately clear from Fig. 3 that almost all measurable exchange times are

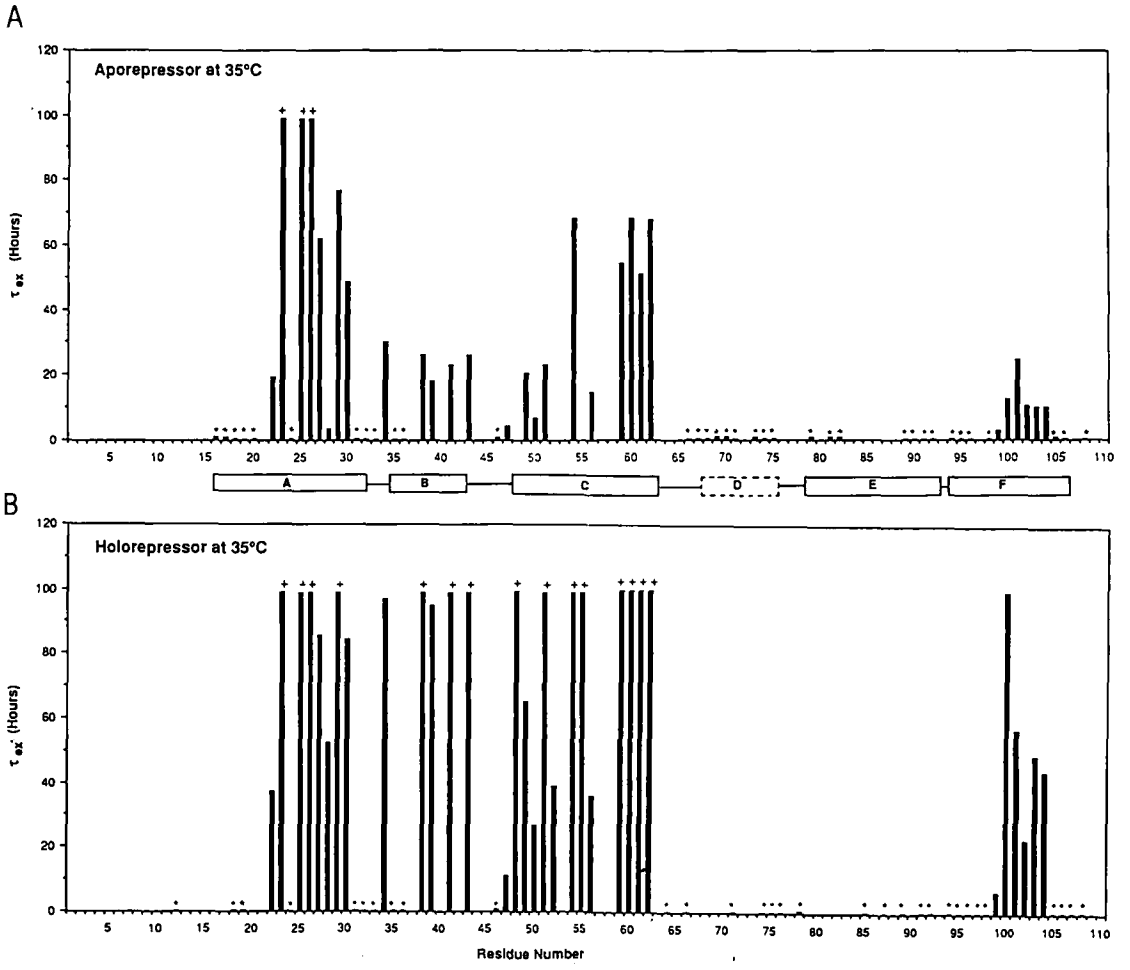

Fig. 3. Lifetimes ($\tau_{ex} = 1/k_{ex}$) of amide protons vs. residue number for (A) aporepressor and (B) holorepressor at 35°C. Actual values are given in Table 2. Lifetimes greater than 100 h are indicated with a + and those shorter than 10 min are indicated with an asterisk (the smallest bars indicate τ_{ex} between 0.001 and 0.1 h and the slightly larger bars correspond to $\tau_{ex} \sim 0.1$ h). The secondary structure determined in solution for the holorepressor (Arrowsmith et al., 1990a) is indicated with solid lines. The residues corresponding to helix D in the crystal structure are shown in dashed lines.

concentrated in helices A, B, C and F, which comprise the hydrophobic core of the dimer. On the other hand, helices D and E, the DNA-binding helix-turn-helix motif, have fast exchange times indicating that these helices are much less stable in both species. Except for residue 34, exchange times in the A-B turn are all fast, indicating that this may be a more flexible turn, whereas the B-C turn appears to be more rigid. Since amide protons in the α-helix are hydrogen bonded to the *i*−4th residue, one would expect the first 4 residues of each helix to have faster exchange rates. The fact that residues 20 and 98 exchange fast points to probable fraying of the N-terminal ends of helices A and F. One curious point in the profile is residue 24, which has a fast exchange rate but is also apparently in the middle of helix A. Although this cannot be fully explained at this time, it

should be pointed out that Asp^{24} is on the surface of the protein. Although ~25% of the resonances are unassigned, it is unlikely that the full profile of exchange times is significantly different from that of Fig. 3 since most of the unassigned peaks exchange rapidly and most are from either the N-terminal or the D-E region. Since proton T_2 measurements have shown that the N-terminal 'arm' is unstructured and highly mobile (Arrowsmith et al., 1989), exchange rates in this region are expected to be fast.

CONCLUSIONS

The amide proton exchange times supported by ^{15}N relaxation studies revealed pronounced differences in the stability of different regions of the *trp*-repressor. The dimeric core of the molecule is relatively compact and homogeneous in terms of the measured parameters in both apo- and holorepressors. On the other hand the DNA-binding region appears less stable and more susceptible to the exchange of its backbone protons with the solvent. The NMR findings reported here are consistent with and amplify information on the stability of the *trp*-repressor obtained by other methods. First, the exchange rates of the backbone protons are on roughly the same time scale as the rate of the monomer-dimer exchange estimated by other methods (Graddis et al., 1988; B. Hurlburt and C. Yanofsky, private communication). This does not prove, but strongly suggests, that the two processes are linked and that both reflect an unraveling of the monomer chain upon dissociation. Binding of the corepressor is known to stabilize the dimer and slow down monomer-dimer exchange by at least an order of magnitude, similar to the difference in exchange time between the two species. More detailed studies of this phenomenon are needed. Second, exchange rates of the backbone protons in the DNA-binding region and in several hinge regions are between *three to five orders of magnitude* faster than in the core region.

Crystallographic data (Lawson et al., 1988) and molecular dynamics (A. Howard, J.M. Guenot and P. Kollman, personal communication) indicate that the helix-turn-helix is an independently flexible domain. The data presented here indicate that it may be even more flexible and less stable than previously thought.

ACKNOWLEDGEMENTS

This research was supported by NIH grants RR-02300 and GM-33385. We thank Dr. Clemens Ainklin of Bruker Instruments for running the 3D HMQC-NOESY, and Dr. Sujata Iyer and Ms. Hong Zhang for preparing labelled protein.

REFERENCES

Altman, R.B. and Jardetzky, O. (1989) In *Methods in Enzymology, Vol. 177*, (Eds., Oppenheimer, N.J. and James, T.L.) Academic Press, New York, p. 218–246.

Arrowsmith, C.H., Carey, J., Treat-Clemons, L. and Jardetzky, O. (1989) *Biochemistry*, **28**, 3875–3879.

Arrowsmith, C.H., Pachter, R., Altman, R.B., Iyer, S.B. and Jardetzky, O. (1990a) *Biochemistry*, **29**, 6332–6341.

Arrowsmith, C.H., Treat-Clemons, L., Szilágyi, L., Pachter, R. and Jardetzky, O. (1990b) In *Die Makromolekulare Chemie* (Macromolecular Symposia, No. 34) (Eds., Höcker, H. and Sedláček, B.) Hüthig & Wepf Verlag, Basel, p. 33–46.

Arrowsmith, C.H., Czaplicki, J., Iyer, S.B. and Jardetzky, O. (1991a) *J. Am. Chem. Soc.*, **113**, 4020–4022.

Arrowsmith, C.H, Pachter, R., Altman, R. and Jardetzky, O. (1991b) *Eur. J. Biochem.*, **202**, 53–66.

Bax, A., Griffey, R.H. and Hawkins, B.L. (1983) *J. Magn. Reson.*, **55**, 301–315.
Graddis, T.J., Klig, L.S., Yanofsky, C. and Oxender, D.O. (1988) *Proteins*, **4**, 173–181.
Hyde, E.I., Ramesh, V., Roberts, G.C.K., Arrowsmith, C.H., Treat-Clemons, L., Klaic, B. and Jardetzky, O. (1989) *Eur. J. Biochem.*, **183**, 545–553.
Kay, L.E., Torchia, D.A. and Bax, A. (1989) *Biochemistry*, **28**, 8972–8979.
Klig, L.S., Carey, J. and Yanofsky, C. (1988) *J. Mol. Biol.*, **202**, 769–777.
Lane, A.N. and Jardetzky, O. (1987) *Eur. J. Biochem.*, **164**, 389–396.
Lawson, C.L., Zhang, R.-G., Schevitz, R.W., Otwinowski, Z., Joachimiak, A. and Sigler, P. (1988) *Proteins*, **3**, 18–31.
Otwinowski, Z., Schevitz, R.W., Zhang, R.-G., Lawson, C.L., Joachimiak, A., Marmorstein, R.Q., Luisi, B.F. and Sigler, P.B. (1988) *Nature*, **335**, 321–329.
Pachter, R., Altman, R.B., Czaplicki, J. and Jardetzky, O. (1991) *J. Magn. Reson.*, **92**, 468–479.
Paluh, J.L. and Yanofsky, C. (1986) *Nucl. Acids Res.*, **14**, 7851–7860.
Schevitz, R., Otwinowski, Z., Joachimiak, A., Lawson, C.L. and Sigler, P.B. (1985) *Nature*, **317**, 782–786.
Zhang, R.-G., Joachimiak, A., Lawson, C.L., Schevitz, R.W., Otwinowski, Z. and Sigler, P.B. (1987) *Nature*, **327**, 591–597.